Advancements in the HELIAS 5-B breeding blanket structural analysis

G. Bongiovì[a]*, A. Häußler[a] and the W7-X team

[a]*Karlsruhe Institute of Technology (KIT), Institute for Neutron Physics and Reactor Technology (INR), Hermann-von-Helmholtz-Platz 1, 76344 Eggenstein-Leopoldshafen, GERMANY*

Within the framework of EUROfusion consortium, the work package S2 aims at developing the HELIcal-axis Advanced Stellarator (HELIAS) as a possible long-term alternative to a tokamak DEMO. From the plasma physics standpoint, the HELIAS 5-B machine is the most promising concept. It is a large 5 field period stellarator reactor directly extrapolated from Wendelstein 7-X. Researches are currently ongoing at KIT in order to attain a preliminary design of the HELIAS 5-B breeding blanket (BB), taking into account as initial input the design experience acquired in the pre-conceptual design phase of the tokamak DEMO BB. To this end, the Helium-Cooled Pebble Bed (HCPB) and the Water-Cooled Lithium Lead (WCLL) BB concepts have been considered, focusing on the investigation of the suitability of their main structural features to the stellarator geometry. In this regard, possible design constraints coming from the Remote Maintenance have to be fulfilled in order to better orient the blanket segmentation. In the present work, a more sophisticated assessment of the BB modules structural behavior has been performed. Attention has been also paid to the refinement of the numerical models so far adopted, investigating the impact of the major assumptions, such as Vacuum Vessel temperature and equivalent Young's Modulus, on the obtained results. To this purpose, dedicated parametric assessment has been carried out and discussed in this work. The obtained results are herewith presented and critically discussed, giving an overview of the follow-up of this activity.

Keywords: HELIAS, stellarator, breeding blanket, thermomechanics, FEM analysis.

1. Introduction

The European roadmap for the realization of fusion energy [1] foresees the demonstration of fusion electricity generation, through the DEMO machine exploitation, by the first half of this century. To this purpose DEMO reactor, conceived according to the tokamak concept, is currently being designed under the umbrella of EUROfusion consortium. In parallel, EUROfusion is also promoting studies on the stellarator concept, considered as the backup solution for the DEMO design. In particular feasibility studies of a HELIcal-axis Advanced Stellarator (HELIAS) [2],[3], equipped with a tritium Breeding Blanket (BB), are currently ongoing.

The studies on HELIAS are in a very early stage compared to the DEMO ones. Nevertheless, preliminary research activities are ongoing at KIT [4]-[8] in order to gather basic results aimed at developing, in a next future, the design of a BB for the HELIAS 5-B machine. In this framework, the present work reports the advancements in the assessment aimed at defining the boundaries for future structural analysis. Firstly, an estimation of the BB segments [9] weight is provided in order to cope with possible Remote Maintenance (RM) restraints. Then, a parametric analysis aimed at verifying the impact of the assumed equivalent Young's Modulus on the BB displacement field has been carried out. Lastly, starting from [4], a more sophisticated assessment of the BB deformation field has been performed, adopting a discrete 3D thermal field for the BB and different Vacuum Vessel temperatures.

The study has been carried out adopting a numerical approach based on the Finite Element Method (FEM) and using the Ansys v.19.1 FEM code.

2. The HELIAS 5-B breeding blanket

A 3D geometric model of half HELIAS-5B field period, including the Vacuum Vessel (VV) and dummy BB segments (full homogenized blocks without internal details), has been considered (Fig. 1).

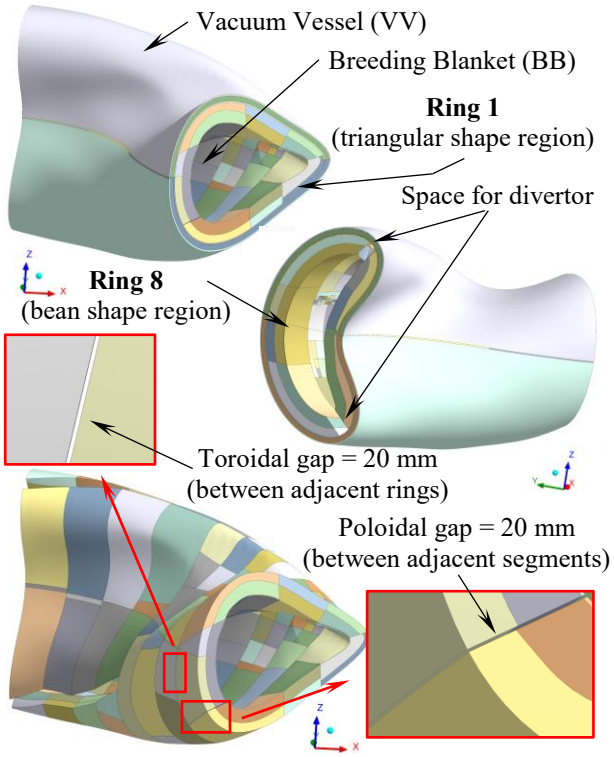

Fig. 1. The HELIAS 5-B BB half torus sector.

author's email: gaetano.bongiovi@kit.edu

It extends toroidally for 36 ° encompassing 8 BB rings which have been designed to be separated by 20 mm gaps. Each ring is composed by 5 BB segments separated, in their turn, by 20 mm gaps along poloidal direction.

The far end rings, namely Ring 1 "triangular shape" region and Ring 8 "bean shape" region, have been separately assessed in this work (Fig. 2). Each ring's geometric model includes the proper portion of VV (divided in inner, shield and outer VV) and, within each segment, the Back Supporting Structure (BSS), the Breeding Zone (BZ), the First Wall (FW) and the 2 mm-thick tungsten armor (W) [7]. In Fig. 2 the segments within each ring have been properly numbered to easily identify them in the following.

Eurofer steel has been considered for BB segments including a W armor facing the plasma, whereas AISI 316 steel has been assumed for the VV , including a steel-water mixture in the VV shielding layer. Temperature dependent thermomechanical properties have been adopted. As homogenized dummy segments are considered, proper equivalent densities have been calculated and adopted in order to consider properly the masses of the structural materials, breeder and coolant. To this end, the same material compositions [10] as the Helium-Cooled Pebble Bed (HCPB) [11]-[13] and Water-Cooled Lithium Lead (WCLL) [14]-[16] DEMO BBs have been assumed.

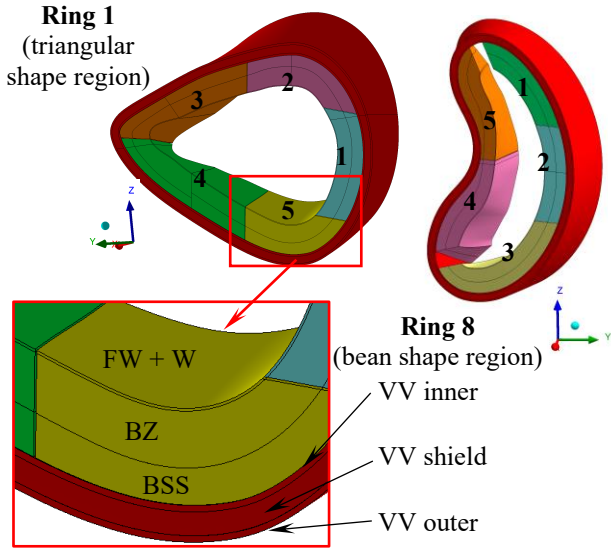

Fig. 2. Ring 1 and Ring 8 geometric models.

3. Estimation of the BB segments weight

The interface between BB and RM plays a crucial role in the BB development, both for DEMO and HELIAS. In particular, RM shall impose a limit on the BB segments weight in order to ensure that the existing tools are capable of safely handling BB segments. Therefore, the weight of the HELIAS 5-B BB segments belonging to Ring 1 and Ring 8 has been estimated considering HCPB and WCLL BB concepts. To this purpose, the above mentioned equivalent densities have been used The other BB concepts presently investigated in EU [17],[18] for the DEMO BB design are not considered in this study. The calculated weights are summarized in Table 1.

Table 1. Estimated BB segments weight [10^3 kg].

Segment	Ring 1		Ring 8	
	HCPB	WCLL	HCPB	WCLL
1	17.4	39.8	27.0	54.7
2	18.6	43.8	25.2	56.0
3	19.9	45.7	30.4	63.3
4	18.8	50.0	17.8	47.4
5	17.4	38.9	16.9	43.9

Results show that, for the HCPB BB, the heaviest segment is segment 3, which is $19.9 \cdot 10^3$ kg heavy in Ring 1 whereas it reaches $30.4 \cdot 10^3$ kg in Ring 8. Higher weights are calculated for WCLL BB concept due to the presence of liquid metal as breeder.

This preliminary evaluation represents the starting point to define the BB-RM interface following a systems engineering approach [19],[20]. In this way a set of design constraints shared by the interfacing system shall be developed in order to better orient the reciprocal design.

4. Parametric study of the equivalent Young's Modulus influence

In the preliminary HELIAS 5-B BB structural analysis reported in [4],[5], temperature dependent Young's Modulus (E) values equal to 10% of the actual ones [21] have been used for the dummy FW, BZ, BSS and VV shield. This assumption aims at making displacement comparable with that of the real structure.

In this work, a parametric study of the assumed E value has been performed to investigate its influence on the displacement field, focusing on the variation of the residual gaps between adjacent BB segments. Temperature-dependent values of E equal to 25%, 50%, 75% and 100% of the actual ones have been considered and results have been compared to the reference case in which E=10% was adopted. To this purpose, Ring 1 and Ring 8 without W armor have been considered to be consistent with the reference case [5]. Only HCPB BB concept has been considered.

4.1 The Ring 1 and Ring 8 FEM models

The same FEM model already developed for the study reported in [5] has been used. Concerning the thermal state, spatially-averaged temperatures of FW, BZ, BSS and VV have been calculated from the DEMO BB thermal analysis and imposed [22]-[24]. In particular, FW has been assumed at 445.8 °C, BZ at 588.0 °C, BSS at 328.5 °C and VV at 200 °C. Regarding gravity load, the global Z direction has been considered as the vertical one (Fig. 2). Lastly, a proper set of mechanical constraints (Fig. 3) has been applied. All the BB components have been considered as mechanically tied.

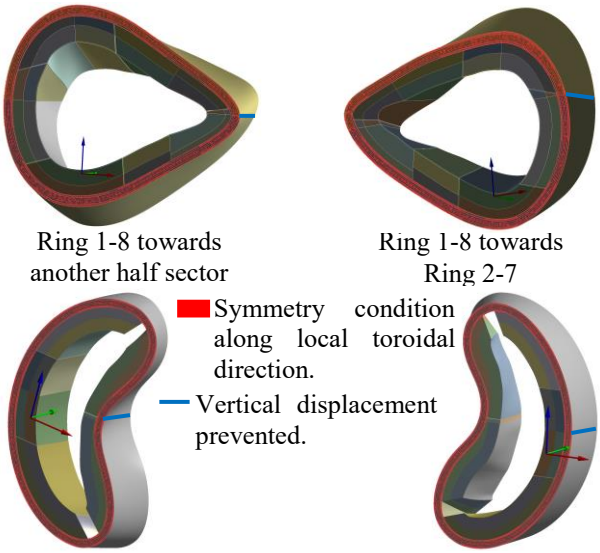

Fig. 3. Mechanical restraints.

4.2 Results of the E parametric analysis

The obtained results in terms of minimum residual gap between adjacent BB segments are reported in Table 2 and Table 3. Negative values (in red) mean that overlapping between neighboring segments occurs.

Table 2. E parametric analysis results - Ring 1.

Minimum residual gap [mm]					
E	Seg 1-2	Seg 2-3	Seg 3-4	Seg 4-5	Seg 5-1
10%	3.097	8.916	4.757	6.003	5.503
25%	3.095	8.539	3.983	5.968	5.792
50%	3.005	8.105	3.209	5.992	5.396
75%	2.899	7.816	2.658	6.043	4.962
100%	2.799	7.609	2.222	6.103	4.584

Table 3. E parametric analysis results - Ring 8.

Minimum residual gap [mm]					
E	Seg 1-2	Seg 2-3	Seg 3-4	Seg 4-5	Seg 5-1
10%	6.917	0.209	-	18.13	-
25%	6.901	-0.465	-	17.92	-
50%	6.391	-1.190	-	17.67	-
75%	5.943	-1.620	-	17.35	-
100%	5.575	-1.903	-	17.05	-

Results have shown that the higher is the considered E, the lower is the minimum residual gap. This means that the condition of E=100 % represents the most conservative case since it causes the narrowest minimum residual gaps. Anyway, this influence is moderate almost everywhere, except for Ring 1 - Seg 3-4 gap where a reduction in minimum residual gap of ~50 %, passing from E=10% to E=100%, has been predicted.

On the basis of these results, two limit scenarios can be identified for the following:

- Less Conservative (LC) scenario: that one where E=10% of the actual ones are assumed.
- More Conservative (MC) scenario: that one where actual E values are assumed.

5. Structural assessment of Ring 1 and Ring 8

In order to obtain a more precise evaluation of the residual gap between adjacent segments within Ring 1 and Ring 8 of the HELIAS 5-B HCPB BB, FEM models adopted for the E sensitivity study have been refined.

5.1 The Ring 1 and Ring 8 refined FEM models

The refined Ring 1 and Ring 8 FEM models include the W armor. Moreover, in order to apply a discrete 3D temperature profile taken from DEMO HCPB BB thermal analysis, all the components of the geometric model shown in Fig. 2 have been purposely sliced (Fig. 4) by means of a dedicated geometry editing campaign.

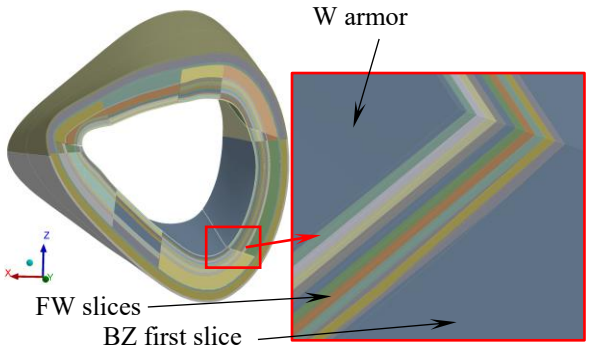

Fig. 4. Ring 1 with sliced components - detail of the FW.

Coherently with the less refined FEM models, linear tetrahedral elements with an element size of 0.05 m have been selected for the mesh (Table 4).

Table 4. Advanced FEM models - mesh features.

Model	Node number	Element number
Ring 1	~1.1M	~4.0M
Ring 8	~1.4M	~5.0M

As to the assumed thermal field, the W armor has been assumed at 551.4 °C. Differently from what previously done, properly calculated average temperatures have been imposed to each FW, BZ and BSS slice instead of to each component. As an example, the assumed FW temperature profile is reported in Table 5. Since the FW is 25 mm thick in all the segments of Ring 1 and Ring 8, the same temperature profile has been imposed to all of them. This is not true for BZ and BSS, whose thicknesses are different from one segment to another and so slightly different temperature profiles have been carried out for them, corresponding to different geometric slicing strategies.

Table 5. FW 3D discrete temperature profile.

r [mm]	T [°C]	r [mm]	T [°C]
0-2.5	544.8	12.5-15	400.2
2.5-5	510.8	15-17.5	403.7
5-7.5	470.2	17.5-20	415.5
7.5-10	431.6	20-22.5	430.6
10-12.5	408.3	22.5-25	442.4

As to VV, its three regions (inner, shield and outer) have been assumed at different temperatures. In particular, due to recent indications coming from DEMO VV design, two different cases have been considered:

- Hot VV case [25]: characterized by VV outer at 180 °C, VV shield at 205 °C and VV inner at 230 °C.
- Cold VV case [26]: characterized by VV outer at 40 °C, VV shield at 65 °C and VV inner at 90 °C.

Lastly, gravity loads has been taken into account considering the Z direction as the vertical one and same boundary conditions depicted in Fig. 3 have been kept. All the components are considered as tied from the mechanical point of view.

Hence, Ring 1 and Ring 8 structural performances have been separately investigated in the following four steady state loading scenarios:

- LC+Hot VV (E=10%, VV between 180 and 230 °C)
- MC+Hot VV (E=100%, VV between 180 and 230 °C)
- LC+Cold VV (E=10%, VV between 40 and 90 °C)
- MC+Cold VV (E=100%, VV between 40 and 90 °C)

5.2 Results

The obtained results in terms of minimum residual gaps are reported, as to Ring 1, in Table 6 and Table 7. Negative values (in red) mean that overlapping occurs, whereas those values lower than 5 mm (assumed as the lowest desirable minimum residual gap to cope with tolerances) are reported in blue. Results clearly show that, in both LC and MC scenarios, the cold VV acts like a rigid wall towards BB and overlapping occurs in all the assessed gaps. In fact, due its low temperature, the cold VV does not accommodate the BB segments thermal expansion. Thus, BB can only move towards the plasma chamber and this effect results in a significant reduction of the gaps between adjacent rings, finally causing overlapping. On the contrary, Hot VV cases are safe. Looking at the third column of the tables, the huge percentage variation of the minimum residual gaps due to the change in VV temperature is reported.

Table 6. Ring 1 results - LC scenarios (E=10%).

Minimum residual gap [mm]			
Segment	LC+Cold VV	LC+Hot VV	Δ%
1-2	-5.938	4.294	172.3%
2-3	-0.846	9.066	1171.4%
3-4	-10.363	4.303	141.5%
4-5	-3.715	8.031	316.2%
5-1	-2.598	2.249	186.6%

Table 7. Ring 1 results - MC scenarios (E=100%).

Minimum residual gap [mm]			
Segment	MC+Cold VV	MC+Hot VV	Δ%
1-2	-5.199	2.952	156.8%
2-3	-2.069	6.791	428.2%
3-4	-11.192	1.510	113.5%
4-5	-4.703	6.340	234.8%
5-1	-1.390	2.203	258.5%

In Table 8, the influence of the E value in case of Hot VV is summarized. As expected, the lowest gaps are obtained for the MC+Hot VV scenario. The maximum percentage variation (~65%) is predicted for segment 3-4.

Table 8. Ring 1 results - Hot VV cases.

Minimum residual gap [mm]			
Segment	LC+Hot VV	MC+Hot VV	Δ%
1-2	4.294	2.952	-31.2%
2-3	9.066	6.791	-25.1%
3-4	4.303	1.510	-64.9%
4-5	8.031	6.340	-21.1%
5-1	2.249	2.203	-2.0%

Similar behavior has been predicted for Ring 8, as shown in Table 9 and Table 10. Here, also for Hot VV condition overlapping occurs between segment 2-3 in case of MC scenario. In Table 11, the influence of E value in case of Hot VV condition is reported. As it can be observed, except for the segment 2-3 gap where overlapping is predicted, the maximum residual gap percentage variation is of 47 % (segment 1-2).

Table 9. Ring 8 results - LC scenarios (E=10%).

Minimum residual gap [mm]			
Segment	LC+Cold VV	LC+Hot VV	Δ%
1-2	-6.621	4.503	168.0%
2-3	-12.514	1.037	108.3%
4-5	-1.168	7.635	753.4%

Table 10. Ring 8 results - MC scenarios (E=100%).

Minimum residual gap [mm]			
Segment	MC+Cold VV	MC+Hot VV	Δ%
1-2	-6.264	2.388	138.1%
2-3	-14.342	-2.976	79.2%
4-5	-1.631	6.081	472.8%

Table 11. Ring 8 results - Hot VV cases.

Minimum residual gap [mm]			
Segment	LC+Hot VV	MC+Hot VV	Δ%
1-2	4.503	2.388	-47.0%
2-3	1.037	-2.976	-387.0%
4-5	7.635	6.081	-20.3%

It has to be noticed that some minimum residual gaps lower than 5 mm are calculated in the Hot VV cases. This suggests to further developing the BB segments design to attain better performances. In particular, these results allow concluding that the VV temperature could represent a major constraint for the development of the HELIAS 5-B BB design. An attachment system is necessary to decouple the VV and BB, reducing the influence of VV deformation on the BB structural performances.

In the end, the total displacement field obtained in MC+Hot VV scenario for Ring 1 and Ring 8 are depicted in Fig. 5 and Fig. 6, where details of the most critical gaps are also shown superimposing the undeformed wireframe to the deformed structure.

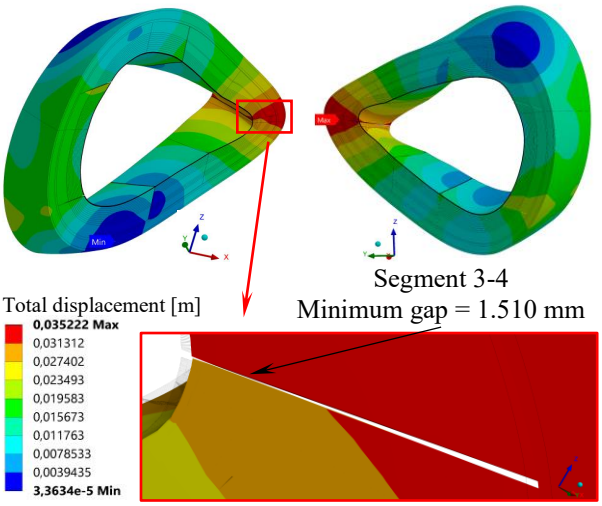

Fig. 5. Ring 1 - MC+Hot VV scenario - Total displacement.

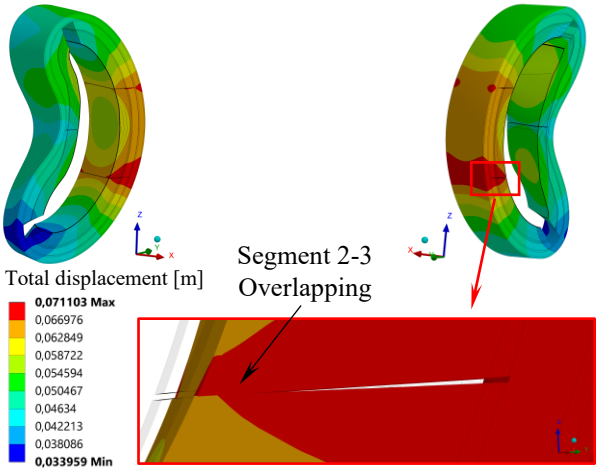

Fig. 6. Ring 8 - MC+Hot VV scenario - Total displacement.

6. Future considerations

The obtained results lead to the conclusion that the next phases of the HELIAS 5-B BB design need some improvements. In particular, large BB models should be developed in order to consider more realistic boundary conditions and, moreover, a proper BB-VV attachment system should be designed to reduce the influence of the VV thermal expansion on the BB structural performances.

As to the first aspect, a 3D CAD model of a whole HELIAS 5-B BB sector, extending for 72 ° along toroidal direction, has been developed (Fig. 7). It includes 16 BB rings toroidally separated by 20 mm-gaps. Each ring still encompasses 5 BB segments poloidally segmented by gaps of 20 mm. Proper structural assessments are ongoing in order to investigate the structural performances of Ring 1 and Ring 8 within this completely characterized geometric configuration.

Concerning the second point, an ITER-like attachment system [27] has been designed for Ring 1 considering M130-type radial pins. A parametric study will be launched to optimize the attachments geometric configuration and assess the BB structural behavior.

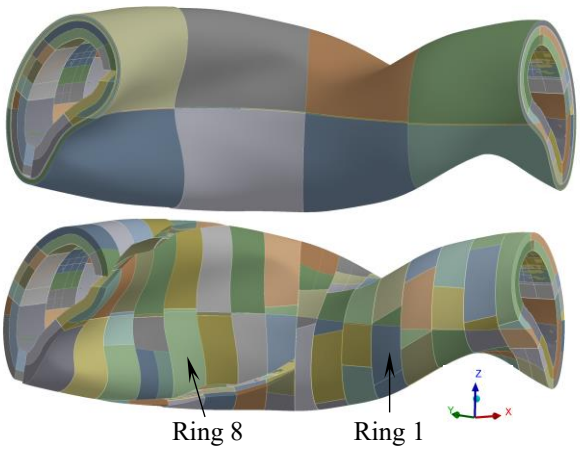

Fig. 7. 3D CAD model of a whole 72° HELIAS 5-B BB sector.

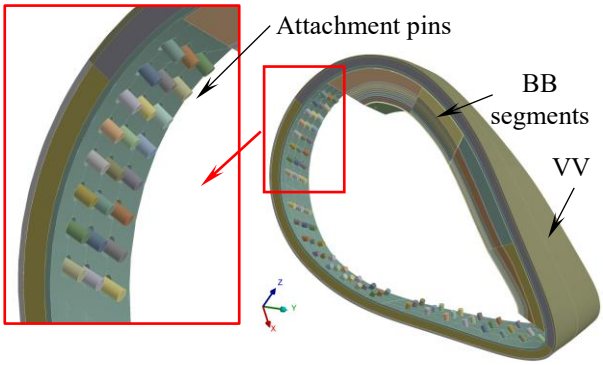

Fig. 8. BB-VV attachment system for Ring 1.

Lastly, the design of the BB internal components (i.e. stiffening plates [28] and FW channels [29]) will be undertaken to attain a fully HELIAS-relevant thermal and mechanical BB characterization.

7. Conclusion

Within the framework of the EUROfusion consortium, a research activity is ongoing at KIT to assess the feasibility of the HELIAS 5-B stellarator fusion reactor BB. Structural calculations of the most representative BB rings have been performed adopting detailed homogenized FEM models. The quite promising outcomes encourage the follow-up of the activity aimed at assessing a whole BB sector, which extends for 72 ° toroidally. Moreover, since a strong influence of the VV temperature on the BB structural performances has been found out, the development of an attachment system devoted to connect BB and VV is crucial, together with the design of the BB segments internal components, to more realistically assess the HELIAS 5-B BB thermomechanical behavior. Lastly, the RM-BB interface should be defined adopting a systems engineering approach in order to consider proper design requirements.

Acknowledgment

This work has been carried out within the framework

of the EUROfusion Consortium and has received funding from the Euratom research and training programme 2014-2018 and 2019-2020 under grant agreement No 633053. The views and opinions expressed herein do not necessarily reflect those of the European Commission.

References

[1] T. Donné et al., European Research Roadmap to the Realisation of Fusion Energy, EUROfusion, 2018 (ISBN 978-3-00-061152-0).

[2] F. Schauer et al., HELIAS 5-B magnet system structure and maintenance concept, Fus. Eng. Des. 88 (2013) 1619-1622.

[3] F. Warmer et al., From W7-X to a HELIAS fusion power plant: On engineering considerations for next-step stellarator devices, Fus. Eng. Des. 123 (2017) 47-53.

[4] G. Bongiovì et al., Preliminary structural assessment of the HELIAS 5-B breeding blanket, Fus. Eng. Des., https://doi.org/10.1016/j.fusengdes.2018.11.027, 2018.

[5] U. Fischer et al., Nuclear design issues of a stellarator fusion power plant with breeder blanket in comparison to tokamaks, paper presented at 27th IAEA Fusion Energy Conference (FEC 2018).

[6] A. Haüßler et al., Use of mesh based variance reduction technique for shielding calculations of the stellarator power reactor HELIAS, Fus. Eng. Des., https://10.1016/j.fusengdes.2019.01.052, 2019.

[7] A. Haüßler et al., Neutronics analyses for a stellarator power reactor based on the HELIAS concept, Fus. Eng. Des., 136, pp. 345-349, 2018.

[8] A. Haüßler et al., Verification of different Monte Carlo approaches for the neutronic analysis of a stellarator, Fus. Eng. Des., 124, pp. 1207-1210, 2017.

[9] G. Bongiovì et al., Multi-Module vs. Single-Module concept: Comparison of thermomechanical performances for the DEMO Water-Cooled Lithium Lead breeding blanket, Fus. Eng. Des., 2018, 136 Part B, pp. 1472-1478.

[10] G. A. Spagnuolo, EFDA_D_2N5LUV v1.0 - Blanket Material Composition For Neutronics - January2017, IDM document ref. 2N5LUV.

[11] F. Hernández et al., A new HCPB breeding blanket for the EU DEMO: Evolution, rationale and preliminary performances, Fus. Eng. Des. 124 (2017) 882-886.

[12] F. Hernández et al., Overview of the HCPB Research Activities in EUROfusion, IEEE Trans. on Pl. Sc. 46 (2018) 2247-2261.

[13] F. Hernández et al., Advancements in the Helium-Cooled Pebble Bed Breeding Blanket for the EU DEMO: Holistic Design Approach and Lessons Learned, Fusion Science and Technology, 75(5), pp. 352-364, 2019.

[14] E. Martelli et al., Advancements in DEMO WCLL breeding blanket design and integration, Int. J. Energy Res., 2018, 42; pp. 27-52.

[15] A. Tassone et al., Recent Progress in the WCLL Breeding Blanket Design for the DEMO Fusion Reactor, IEEE Trans. on Pl. Sc., 2018, 46, pp. 1446-1457.

[16] A. Del Nevo et al., Recent progress in developing a feasible and integrated conceptual design of the WCLL BB in EUROfusion project, Fus. Eng. Des. (2019), DOI: 10.1016/j.fusengdes.2019.03.040.

[17] J. Aubert et al., Status of the EU DEMO HCLL breeding blanket design development, Fus. Eng. Des., 2018, 136, Part B, 1428-1432.

[18] D. Rapisarda et al., Conceptual Design of the EU-DEMO Dual Coolant Lithium Lead Equatorial Module, IEEE Trans. on Pl. Sc., 2016, 44, pp. 1603-1612.

[19] G. Bongioví et al., Systems engineering activities supporting the heating & current drive and fuelling lines systems integration in the European DEMO breeding blanket, Fus. Eng. Des., 147, 111265, 2019.

[20] G. A. Spagnuolo et al., Systems Engineering approach in support to the breeding blanket design, Fus. Eng. Des., https://doi.org/10.1016/j.fusengdes.2018.11.016, 2018.

[21] P. A. Di Maio et al., Structural analysis of the back supporting structure of the DEMO WCLL outboard blanket, Fus. Eng. Des. 124 (2017) 944-947.

[22] G. Zhou et al., Transient thermal analysis and structural assessment of an ex-vessel LOCA event on the EU DEMO HCPB breeding blanket and the attachment system, Fus. Eng. Des., 136, 34-41, 2018.

[23] P. A. Di Maio et al., On the thermo-mechanical behavior of DEMO water-cooled lithium lead equatorial outboard blanket module, Fus. Eng. Des. 124 (2017) 725-729.

[24] G. Federici et al., European DEMO design strategy and consequences for materials, Nucl. Fusion 57 (2017), 092002.

[25] C. Bachmann, PDD-Plant Description Document v.1.3, https://idm.euro-fusion.org/?uid=2KVWQZ.

[26] C. Bachmann, PDD-Plant Description Document v.1.5, https://idm.euro-fusion.org/?uid=2KVWQZ.

[27] ITER Blanket Design Description Document, IDM UID EBUDW3, v.1.1, 2013

[28] P. A. Di Maio et al., On the effect of stiffening plates configuration on the DEMO Water Cooled Lithium Lead Breeding Blanket module thermo-mechanical behavior, Fus. Eng. Des., https://doi.org/10.1016/j.fusengdes.2019.03.163, 2019.

[29] P. A. Di Maio et al., On the optimization of the first wall of the DEMO water-cooled lithium lead outboard breeding blanket equatorial module, Fus. Eng. Des., 109-111(PartA), pp. 335-341, 2016.